A cryogenic optical feedthrough using polarisation maintaining fibers

Speake, Clive; Nelson, Michaela; Collins, Chris

DOI:
10.1063/1.4943678

Document Version
Publisher's PDF, also known as Version of record

Citation for published version (Harvard):
Speake, C, Nelson, M & Collins, C 2016, 'A cryogenic optical feedthrough using polarisation maintaining fibers', Review of Scientific Instruments, vol. 87, no. 3, 033111. https://doi.org/10.1063/1.4943678

A cryogenic optical feedthrough using polarization maintaining fibers

M. J. Nelson, C. J. Collins, and C. C. Speake

Citation: Review of Scientific Instruments **87**, 033111 (2016); doi: 10.1063/1.4943678
View online: https://doi.org/10.1063/1.4943678
View Table of Contents: http://aip.scitation.org/toc/rsi/87/3
Published by the American Institute of Physics

A cryogenic optical feedthrough using polarization maintaining fibers

M. J. Nelson, C. J. Collins, and C. C. Speake
School of Physics and Astronomy, University of Birmingham, Edgbaston, Birmingham B15 2TT, United Kingdom

(Received 30 September 2015; accepted 29 February 2016; published online 25 March 2016)

Polarization maintaining optical fibers can be used to transmit linearly polarized light over long distances but their use in cryogenic environments has been limited by their sensitivity to temperature changes and associated mechanical stress. We investigate experimentally how thermal stresses affect the polarization maintaining fibers and model the observations with Jones matrices. We describe the design, construction, and testing of a feedthrough and fiber termination assembly that uses polarization maintaining fiber to transmit light from a 633 nm HeNe laser at room temperature to a homodyne polarization-based interferometer in a cryogenic vacuum. We report on the efficiency of the polarization maintaining properties of the feedthrough assembly. We also report that, at cryogenic temperatures, the interferometer can achieve a sensitivity of 8×10^{-10} rad/$\sqrt{\text{Hz}}$ at 0.05 Hz using this feedthrough. © *2016 AIP Publishing LLC.* [http://dx.doi.org/10.1063/1.4943678]

I. INTRODUCTION AND MOTIVATION

Polarization Maintaining (PM) fibers are single-mode optical fibers that, when correctly implemented, maintain the state of linear polarization (SOP) of an input light source over considerable distances.[1] PM fibers are widely used, but their use in cryogenic environments has been limited by their sensitivity to temperature changes. The Inverse Square Law (ISL) experiment[2] aims to test gravity at a range of 14 μm in order to be sensitive to possible modifications due to large extra dimensions.[3] The current project, which follows on from a previous experiment that used a magnetically levitating spherical superconducting torsion balance,[4] uses twelve superconducting coils to levitate and control a triangular prism-shaped torsion balance on top of which is mounted an assembly of test masses, comprising alternating radial gold and copper spokes. The gravitational torque on the test masses produces an angular rotation of the torsion balance. In order to achieve the goal of the ISL project, a detector with a sensitivity of 8×10^{-10} rad/$\sqrt{\text{Hz}}$ at a frequency of 0.05 Hz is required. Above this level, the readout noise would begin to dominate over the seismic noise, which otherwise dominates. Mechanical thermal noise should not be significant, due to the experiment's cryogenic operation. A suitable angular interferometer, ILIAD, has already been developed for use at room temperature.[5] This is a polarization-based homodyne interferometer which operates at 1550 nm and is fed with a PM fiber. This paper describes the development of a cryogenic PM fiber-feed which allows a version of this interferometer to be used in a vacuum at 4 K.

There are many applications of PM fibers in fiber communications and in-line optics[9] and the techniques discussed in this paper would be relevant to cryogenic applications of these technologies. It could also enhance the sensitivity of atomic force microscope measurements of surfaces at low temperatures, by allowing a more precise interferometer to be used.

The paper is set out as follows: Section II describes the optics involved in a simple system to deliver polarized light through a PM fiber and uses Jones Matrices to model the system analytically. Section III describes the experimental observation of the performance of a standard fiber vacuum feedthrough and termination in a cryogenic environment. Section IV describes an improved low-stress system and its observed performance.

II. FIBER CHARACTERIZATION

A PM fiber, first proposed in 1978,[6] is a single mode optical fiber with a strong birefringence caused by a built in asymmetry[7] that can be due to an elliptical core (shape birefringence) or mechanical stress (stress birefringence). The birefringence produces a difference between the phase speeds of each of the two orthogonal planes of polarization that can propagate along the fiber. The axis along which the refractive index is maximized (minimized) is referred to as the slow (fast) axis. If the difference in refractive index is much larger than random changes in birefringence caused by bending, temperature, and other environmental effects, a PM fiber can be configured to maintain the SOP of the incident light over considerable distances.[8]

The birefringence of a PM fiber is defined as the difference between the refractive indices of the slow and the fast axes, $\delta n = n_s - n_f$. When linearly polarized light is launched into a PM fiber with its electric field aligned at a general angle to its axes, the difference in phase velocities between components aligned with the fiber axes (eigenmodes) causes the resultant net polarization to vary along the length of the fiber. The difference in phase, $\Delta\phi$, between the two polarization states at a point a distance, L, along the fiber is

$$\Delta\phi = \frac{2\pi}{\lambda}\,\delta n\, L, \tag{1}$$

where λ is the wavelength of the light. For the two eigenmodes to be in phase, $\Delta\phi = m2\pi$, where m is an integer. The length that satisfies this condition with $m = 1$ is known as the beat length, L_b, where $L_b = \frac{\lambda}{\delta n}$. The greater the birefringence

within the fiber, the greater the difference between the two velocities and the shorter the beat length.[11]

Ideally, when light is launched into a PM fiber, all the light that is launched into a particular axis will remain there, with no leakage. In practice, this is difficult to achieve and there will always be some light scattered into the orthogonal axis by intrinsic impurities and extrinsic stresses on the fiber. For a perfectly linearly polarized input beam, any misalignment of the input beam will result in some of the light being launched in the orthogonal axis, so accurate alignment of the light with one of the fiber axes (conventionally the light is aligned with the slow axis) is necessary. If the polarization is not aligned accurately, then even very small changes in the environmental conditions will cause fluctuations in the SOP of the output light. Phase shifts of $\Delta\phi = 2\pi$ have been measured in fibers where a 19 cm long fiber is stretched by as little as 70 μm (0.037% increase in length) and for temperature changes of about 10° in a 10 cm length of fiber.[12]

The fiber being used for the ILIAD interferometer is a "Panda" fiber that uses stress-induced birefringence and it connects a laser at room temperature to the experiment at 4 K. The fiber experiences large temperature changes and is also subjected to mechanical stress where it passes through vacuum flanges. A reduction in temperature causes the birefringence of the fiber to increase[13] which decreases the beat length. Cooling of the feedthroughs and any other parts in contact with the fiber may also indirectly stress the fiber and affect the birefringence due to differential thermal expansion between materials. Thus it is important to quantify how the fiber will behave when cooled and stressed so that these changes can be reduced and the SOP of the output light can be understood and controlled. It would be difficult to predict these effects from finite element simulations. This is partly due to the different size scales present within the fiber and the surrounding components, but also because azimuthally symmetric stress should not cause mixing between the two linear polarizations. As most feedthroughs and other components to which the fiber is connected are designed to be circularly symmetric, one then has to guess how imperfectly the fiber is held. It was more instructive to experimentally measure the polarization mixing and extinction caused by thermally induced mechanical stress on the fiber. Section II A will describe the experiments that have been performed in order to understand how the various stresses on the 633 nm fiber will influence the SOP of the light entering the interferometer. Nevertheless it is instructive to note the approximate levels of stress that may be of importance when working with PM fibers: the peak value of the intrinsic stress field is about 70 MPa according to Ref. 9. We can estimate the stress applied to a fiber as follows: if we imagine that a silica fiber is inserted into a hole in a copper flange of such diameter that it just fits at room temperature, and we take the diameter of the flange to be much larger than the diameter of the fiber, the stress applied to the fiber on cooling is given by[10]

$$\sigma = \left(\frac{\Delta L}{L}(\mathrm{Cu}) - \frac{\Delta L}{L}(\mathrm{SiO_2})\right) \times \left(\frac{1}{E_{\mathrm{Cu}}}(1+\nu_{\mathrm{Cu}}) + \frac{1}{E_{\mathrm{SiO_2}}}(1-\nu_{\mathrm{SiO_2}})\right)^{-1}, \quad (2)$$

where $\frac{\Delta L}{L}(\mathrm{Cu})\left(\frac{\Delta L}{L}(\mathrm{SiO_2})\right)$ represents the linear thermal contraction between room temperature and the temperature in question for copper (silica), $E_{\mathrm{Cu}}\left(E_{\mathrm{SiO_2}}\right)$ is the Young's Modulus of copper (silica), and $\nu_{\mathrm{Cu}}\left(\nu_{\mathrm{SiO_2}}\right)$ is the Poisson's ratio for copper (silica).

Putting in values for the material constants, we find that the stress at 77 K and 4 K is given by 144 MPa and 131 MPa, respectively. ANSYS simulations reproduce the predictions of this analytical model to within a few percent. This stress does not necessarily act against the stress asymmetry which produces the birefringence in the fibre and may be reduced by the presence of a glue layer between the metal flange and the fibre. Nevertheless, it shows that the stress involved in cooling is of a comparable magnitude to that producing the stress-induced birefringence, and so might be expected to significantly affect it.

A. Experimental setup

In order for the PM fiber to act to maintain SOP of the output light, the input light needs to be launched into one of the two axes of stability of the fiber. Two methods are commonly used to align the light from a polarised laser to the axis of a PM fiber which are, first, to use a halfwave plate to rotate the plane of polarization of the laser light and, second, to rotate the laser or the fiber directly into the correct plane. The variation of the fiber's birefringence with temperature can be exploited to establish how well-aligned the laser is with the fiber, using the experimental setup illustrated in Figure 1. At each input angle a section of fiber wound around a reel can be placed over a Liquid Nitrogen (LN2) bath. The fiber is wound loosely around the reel, so should not experience stress due to the thermal contraction or warping of the reel. While the ISL experiment is to be carried out at Liquid Helium (LHe) temperatures, the majority (more than 90% as shown in Equation (2)) of thermal contraction and other mechanical effects occur between room temperature and LN2 temperature. As it is much easier to cool components to LN2 temperature, this was used for the majority of the smaller experiments described in this section and in Section IV, in which individual components are cooled separately.

As the fiber cools, the birefringence will change and any light in the orthogonal axis will beat with the light in the launch axis and cause oscillations in the polarization of the light exiting the fiber. When this light is subsequently passed

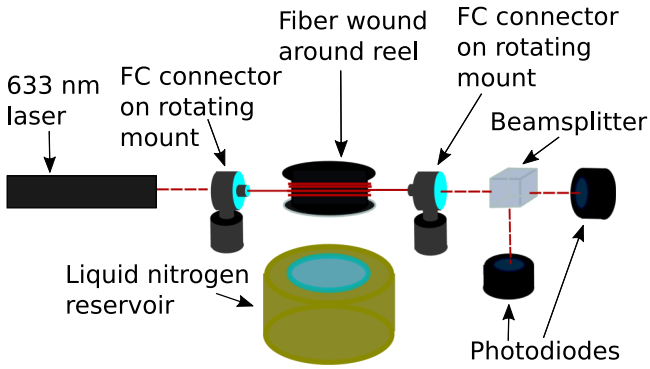

FIG. 1. Experimental setup for cooling a PM fiber.

through a fixed linear polarizer, this translates into variations in the resultant intensity. We refer to this effect as Thermally Induced Birefringent Interference (TIBI). These oscillations can be observed with a polarizer and one or more photodiodes and their amplitude will be at minimum when the polarization of the input laser light is aligned with one of the two axes.

While these TIBI oscillations could in principle be eliminated by controlling the temperature of the fiber, this is often impractical. For instance, in the ISL experiment, the vacuum chamber itself has a servo system which can be engaged to stabilise the temperature, but this would not extend to the whole length of the fiber, extending through the Dewar to the room temperature flange. It would be possible to use the output from the fiber itself to operate a servo system to keep the transmitted component at a maximum of one of the oscillations, but this solution adds significant complexity. Instead, a passive solution was sought in which the size of the oscillations was minimised.

Two methods are commonly used to align the plane of polarization of the light from a laser to an axis of a PM fiber. First, a half-wave plate can be used to rotate the plane of polarization of the laser light, and, second, the fiber and the laser can be mechanically rotated with respect to each other. Both methods of launching the light into the fiber were tested to see how well the TIBI could be minimized; first two different half-wave plates were tested and it was found that they both allowed a small amount of light into the other axis (indicating that they did not perfectly maintain linear polarization) and thus interference was always observed when the fiber was cooled. Aligning the fiber directly with the laser proved to be a better method and a greater proportion of the light could be launched into the desired axis. For the latter method, it was possible to locate the axis accurately enough that almost no light was launched into the orthogonal axis.

The experimental setup shown in Figure 1 was used to further understand how the stability of the output light depended on the orientation of the input light with respect to the fiber and the output polarizer. Two data sets were taken and in both cases, the input collimator attached to the fiber was rotated through an angle θ_1 and the output orientation of the fiber, θ_2, was fixed with respect to the polarizing beam splitter. At each input angle, the section of fiber wound around the reel was placed over the liquid nitrogen bath, thus cooling the fiber and causing TIBI. The output intensity of the fiber was recorded by the two photodiodes and the results are shown in Figure 2. At each measured combination of input and output rotation angles, the fiber is cooled, and the amplitude of the oscillations in the output is recorded. The fiber was cooled in vapour from the LN2, and the exact temperature reached was not known in each case. It could be estimated by counting the number of oscillations and comparing this to the number observed when a length of fiber was completely immersed in LN2; generally it would lie between 150 K and 250 K, which corresponds to several tens of TIBI oscillations. However, the amplitude of the oscillations for the "free" (i.e., not rigidly connected to a material with different thermal expansion coefficient) fiber did not show any significant dependence on temperature. As long as several oscillations were excited, the amplitude could be recorded.

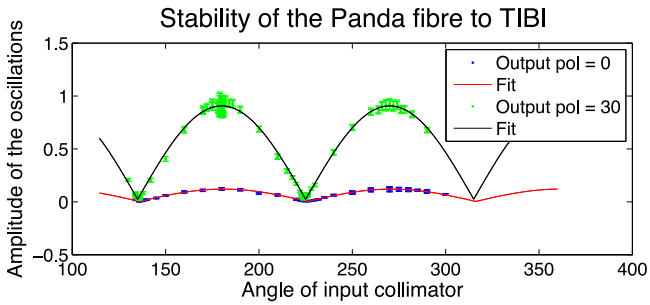

FIG. 2. Amplitude of TIBI oscillations as a function of input angle for two different output collimator angles: Approximately zero (green data points) and 30° (blue data points) alongside fitted rectified sine waves (solid curves).

The amplitude shown is as a fraction of the transmitted amplitude observed without the final beam-splitter present, and so should not be affected by changes in the amplitude of the laser or of the coupling of the laser into the fiber. For the first data set, the output of the fiber was roughly aligned with the output Polarizing Beam-Splitter (PBS) ($\theta_2 \simeq 0$) and for the second data set, the orientation was $\theta_2 \simeq 30°$. The amplitude of oscillations will in general vary slightly during one cooling experiment. The uncertainties shown come from measuring the minimum and maximum amplitude of oscillations during one cooling and are in general approximately proportional to the amplitude of the oscillations.

As the input is rotated, areas of maximum stability and instability are observed periodically, with a period of $\pi/2$, corresponding to the fast/slow axis (maximum stability) and 45° between the axes (maximum instability). From these results, it is not possible to distinguish between the fast and slow axis. The amplitude of the oscillation, A_{TIBI}, as a function of the input angle, θ_1, was fitted to a rectified sine wave,

$$A_{TIBI} = A_0 + a\,|\sin(2(\theta_1 + \theta_0))|, \tag{3}$$

using a nonlinear least squares method. A_0 is the minimum amplitude of oscillations, θ_0 is the input angle at which the oscillations are minimized, and a is the amplitude of the θ-dependent part of the oscillations. This procedure was carried out for two different angles of the output of the fiber with respect to the polarizer, one as close as could be achieved to 0° and one at approximately 30°. Table I shows the fitted parameters and their respective fitting and measurement errors.

TABLE I. Measured fit parameters.

Output polarizer angle θ_2	0°	30°
Min. amplitude , A_0	0.0033	0.024
Fitted error	0.0012	0.0022
Measurement error	0.01	0.01
Phase, θ_0	223.90	224.95
Fitted error	0.22	0.06
Measurement error	0.5	0.5
Amplitude, a	0.1165	0.8820
Fitted error	0.0017	0.0036
Measurement error	0.0125	0.05

B. Comparison with Jones matrix calculations

The experimental setup shown in Figure 2 can be modeled using Jones matrices. The input light is represented by the 2×1 Jones vector,

$$\mathbf{E} = \begin{pmatrix} E_x \\ E_y \end{pmatrix} = \begin{pmatrix} E_{0x} e^{i\delta_x} \\ E_{0y} e^{i\delta_y} \end{pmatrix}, \tag{4}$$

where $\delta_{x,y}$ are arbitrary phase angles.

Polarizing elements acting on the input light are represented by 2×2 Jones matrices. The output light is found by taking the product of the Jones matrix and the Jones vector. In the calculation, the fiber is represented by the matrix $J_F(\phi)$ corresponding to a wave-plate ($E_{0x} = E_{0y} = 1$) with a phase shift of $\frac{\phi}{2}$ along the fast axis and $\frac{-\phi}{2}$ along the slow axis,

$$\mathbf{J}_F(\phi) = \begin{pmatrix} e^{\frac{i\phi}{2}} & 0 \\ 0 & e^{\frac{-i\phi}{2}} \end{pmatrix}. \tag{5}$$

The angle between the laser and the input of the fiber axes, θ_1, is represented by the rotation matrix, $\mathbf{J}_R(\theta_1)$, where

$$\mathbf{J}_R(\theta) = \begin{pmatrix} \cos\theta & -\sin\theta \\ \sin\theta & \cos\theta \end{pmatrix}. \tag{6}$$

The Jones matrix for the polarizer, $\mathbf{J}_P$, is represented as in Ref. 1,

$$\mathbf{J}_P = \begin{pmatrix} 1 & 0 \\ 0 & 0 \end{pmatrix}. \tag{7}$$

The angle between the laser and the output polarizer is given by θ_2. Thus, if $\theta_1 = \theta_2 = 0$, both the fiber and the PBS would be aligned to the plane of the input light. The matrix calculation can be written as

$$\mathbf{E}_{Out} = \mathbf{J}_R(-\theta_2)\mathbf{J}_P\mathbf{J}_R(\theta_2)\mathbf{J}_R(\theta_1)\mathbf{J}_R(-\theta_1)\mathbf{J}_F\mathbf{J}_R(\theta_1)\mathbf{E}_{In}. \tag{8}$$

We observe experimentally that the oscillation will typically evolve through tens of periods as a section of fiber is cooled in nitrogen vapour indicating that ϕ varies over a range larger than 2π. We then move to a different value of θ_1 or θ_2 and again vary ϕ. For an input light with unit intensity in the x-polarization, we find that the output intensity in this polarization (i.e., the "transmitted" component; the other component will behave similarly) is equal to

$$E_x = e^{i\phi/2}\cos\theta_1\cos^2\theta_2 + e^{-i\phi/2}\cos\theta_1\cos\theta_2\sin\theta_2, \tag{9}$$

while the output in the y-axis is

$$E_y = e^{i\phi/2}\sin\theta_1\cos^2\theta_2 + e^{-i\phi/2}\sin\theta_1\cos\theta_2\sin\theta_2. \tag{10}$$

Focusing on E_x, we find that, for fixed θ_1, if $-\pi/4 \le \theta_2 \le \pi/4$, then as the phase, ϕ, varies between 0 and 2π, the intensity observed will vary sinusoidally between $\cos\theta_1\cos^2\theta_2 + \cos\theta_1\cos\theta_2\sin\theta_2$ and $\cos\theta_1\cos^2\theta_2 - \cos\theta_1\cos\theta_2\sin\theta_2$. The amplitude of the oscillation, A_1, will therefore be equal to

$$A_1 = 2\cos\theta_1\cos\theta_2\sin\theta_2. \tag{11}$$

If $\pi/4 \le \theta_2 \le 3\pi/4$, then as the phase, ϕ, varies between 0 and 2π, the intensity observed will vary between $\cos\theta_1\cos\theta_2\sin\theta_2 - \cos\theta_1\cos^2\theta_2$ and $\cos\theta_1\cos^2\theta_2 + \cos\theta_1\cos\theta_2\sin\theta_2$. The amplitude of the oscillation, A_2, will therefore be equal to

$$A_2 = 2\cos\theta_1\cos^2\theta_2. \tag{12}$$

For general values of θ_2, the amplitude of the oscillations will be equal to the minimum of A_1 and A_2.

The amplitude of the oscillations as a fraction of the maximum intensity observed for a fixed value of θ_2, A_{Rel}, will be equal to

$$A_{Rel} = Min\left(\frac{1}{1+\tan\theta_2}, \frac{1}{1+\cot\theta_2}\right). \tag{13}$$

In the experiments, we are not observing the phase of the oscillations but only their amplitude, therefore the oscillation amplitude, when plotted as a function of θ_1 for fixed θ_2, will take the form of a rectified sine wave. This can be seen in the experimental results in Figures 4-7. The observed amplitude of the oscillations in the two experimental results is best fitted to orientations of the PBS of approximately 3° and 31°. The Jones matrix calculations are for an ideal fiber and if the PBS is at 0°, no oscillations should be seen regardless of the input angle θ_1. Further experimental measurements around $\theta_1 = 0°$ confirm that the fiber is not ideal, and even with the best alignment, TIBI with a maximum amplitude of 0.1% is still observed. For a fiber that is 20 m long, this corresponds

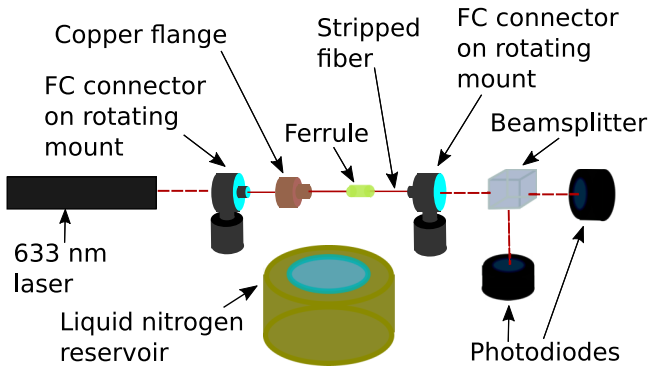

FIG. 3. Experimental setup for cooling vacuum flange and ferrule.

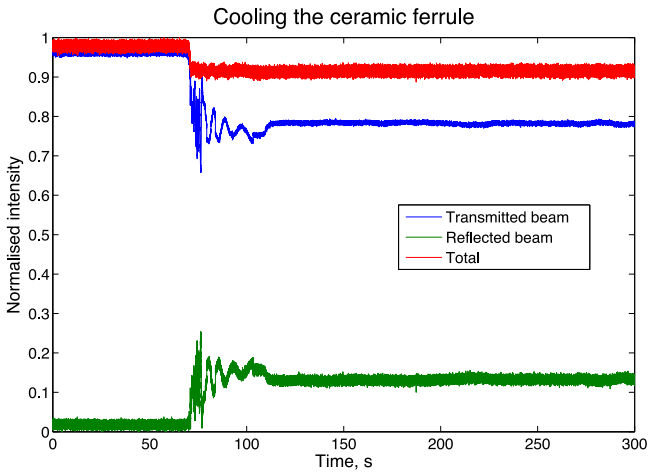

FIG. 4. Changes in the reflected and transmitted light as the ceramic ferrule is cooled in liquid nitrogen. Total drop in intensity of 7% is observed and a maximum 30% change in intensity for the transmitted component.

to an intrinsic scattering of approximately 0.0005%/m; for the 4 m fiber used in the ISL experiment, this will be about 0.002%.

C. Effect of winding around the reel

Bending the optical fiber will produce an anisotropic strain in the fused quartz material and will alter its refractive index and birefringence. The changes in the refractive index in the x and y directions of an originally isotropic medium, Δn_x and Δn_y, are given by[1]

$$\begin{aligned} \Delta n_x &= \frac{n^3}{4}(p_{11} - 2\nu p_{12})\left(\frac{r}{R}\right)^2, \\ \Delta n_y &= \frac{n^3}{4}(p_{12} - \nu p_{12}\nu p_{11})\left(\frac{r}{R}\right)^2 \end{aligned} \tag{14}$$

with r the radius of the fiber, R the radius of curvature of the reel, ν is Poisson's Ratio, and p_{11} and p_{12} are two terms of the photoelastic tensor. Typically for silica, $\nu = 0.16$, $n = 1.47$, $p_{11} = 0.121$, and $p_{12} = 0.270$ giving

$$\delta n = \Delta n_x - \Delta n_y = -0.133\left(\frac{r}{R}\right)^2 \tag{15}$$

which for a radius of curvature of 0.1 m and fiber radius of 125 μm yields $\delta n \simeq 2 \times 10^{-7}$ which is approximately 1700 times smaller than a typical $\Delta n_{fast} - \Delta n_{slow} = 3.5 \times 10^{-4}$ of a PM fiber. Thus the wrapping of the fiber around a reel should have no observable impact on our results.

III. OBSERVED CRYOGENIC PERFORMANCE OF STANDARD FIBER VACUUM FEEDTHROUGHS AND TERMINATION

Optical fibers remain flexible at low temperatures,[14] and for PM fibers, their birefringence increases as temperature decreases.[13] This may lead to an assumption that their use at cryogenic temperatures is straightforward. However, their ability to maintain polarization relies on accurate alignment of the input light with the fiber axes and how well this is maintained as the fiber is cooled. As Section II demonstrates, the fluctuations in the SOP caused by changes in temperature can be almost eliminated by accurately aligning the input light with the fiber axis and the output light with the polarizing optics. However stress on the fiber can cause light to scatter into the orthogonal axis and if this becomes significant then, as the temperature changes, TIBI will cause the intensity of the preferred polarization state to become unstable. The PM fiber which is used in the ISL experiment experiences stress in two areas as a result of a change in temperature. The first is where the fiber passes through a cryogenic vacuum feedthrough and second is within the last 10 mm of the fiber where it is terminated with a connector. In both these places, the fiber is in mechanical contact with another material of different thermal expansion coefficient, namely, copper in the feedthrough and the ceramic Zirconium Dioxide of the ferrule in the connector.

The first attempt to test the ILIAD cryogenically used a fiber feed where the fiber was glued into the ferrule and the feedthrough with an epoxy specifically chosen to reduce the stress on the fiber when cooled. However, despite accurate alignment of the laser, fiber, and optics, large (over 50%) fluctuations were observed in the intensity of the light reaching the interferometer.

In order to ascertain how the cooling of the fiber feed (specifically the feedthrough and the ferrule) was affecting the stability of the output light, a test fiber was manufactured. The test fiber assembly was identical to the fiber feed which had been used in the previous cryogenic experiment except that an additional ferrule was placed approximately 30 cm from the end of the fiber and glued into place, as shown in Figure 3. In order to do this, the last 30 cm of fiber is needed to be stripped entirely of its acrylate buffer layer (250 μm) down to the glass cladding (125 μm) so that the ferrule (inside diameter 126 μm) could be slid into place. The unbuffered section is delicate and must be handled carefully. Using this setup, it was possible to cool both the feedthrough and the ferrule independently or simultaneously. The input and output of the fiber could be maintained at room temperature and the optics were thus not affected by condensing and freezing air from the atmosphere. This technique enabled us to test the fiber feed assembly without the need for cooling the complete experimental cryostat. With the laser aligned to the fiber axis, the feedthrough and ferrule were cooled. In this case, we wanted to cool the feedthrough and ferrule to LN2 temperature, rather than to some arbitrary lower temperature, as was the case when cooling the fiber. This was achieved by cooling the components as far as possible in LN2 vapour, as with cooling the fiber (in order to minimise thermal shock), then immersing them in LN2. The output light was passed through a polarizing beam-splitter, and two polarizations of the output light (referred to henceforth as the reflected and transmitted light) were recorded with two photodiodes.

The results in Figures 4 and 5 are two examples obtained when the ceramic ferrule is cooled to liquid nitrogen temperature. Figure 4 shows an overall drop in intensity of 7% compared with 8.3% in Figure 5. There was also a change in the intensities of the two polarizations of the light in the fiber. The upper and lower curves in Figure 4 show that the transmitted intensity changed from a maximum of 96% at room temperature to a minimum of 66%, finally settling at

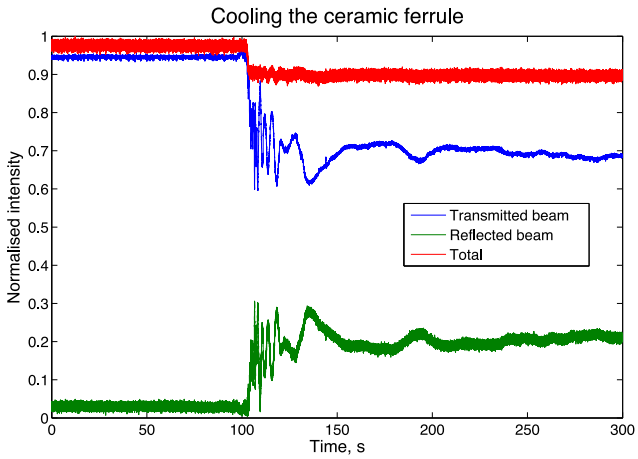

FIG. 5. Changes in the reflected and transmitted light as the ceramic ferrule is cooled in liquid nitrogen. Total drop in intensity of 8.3% is observed and a maximum 36% change in intensity for the transmitted component.

78.5%. From Figure 5, the transmitted polarization reached a minimum of 60%, a drop of 36%, and did not completely settle within the time of the recording but was 69% at 300 s. The final SOP of the cooled fiber depends on the fiber length and the temperature change and could be anywhere between the observed maximum and minimum values. As there are a large number of oscillations, it would be expected that the final phase would be, to a good approximation, uniformly distributed. A number of cooling cycles seemed to confirm this, though in general the temperature would not be sufficiently stable in the cold state for a definite value of the phase to be recorded. The two cooling experiments shown in Figures 4 and 5 represent examples in which the temperature did appear to have levelled off, though Figure 5 still showed some drift.

Cooling the feedthrough also resulted in a change of polarization of the light in the fiber, with up to about 15% of the light scattering into the other polarization, but it was not responsible for any overall loss in intensity, as shown in Figure 6.

The combination of the fluctuations caused by the differential thermal expansion in the ferrule and the feedthrough is enough to account for the change in the SOP of the light observed when the ILIAD was tested cryogenically.

IV. MODIFIED LOW-STRESS VACUUM FIBER FEEDTHROUGHS AND TERMINATION

The results in Figures 4–6 show that over 50% of the total intensity of the polarized light exiting the fiber at room temperature could be scattered into the orthogonal polarization as the fiber is stressed during cooling. Most of this scattering was due to the ceramic ferrule, but some was due to the copper feedthrough, and methods for reducing the stress in both were investigated. The most obvious way to reduce the stress caused by the ceramic ferrule is to replace the ceramic with glass, thus better matching the thermal expansion of the fiber. A test fiber was made up similar to the one shown in Figure 3 but with a glass ferrule instead of a ceramic one. The glass ferrule was silicate bonded onto the fiber, thus eliminating the need for epoxy. This ferrule was cooled in the same way as the ceramic

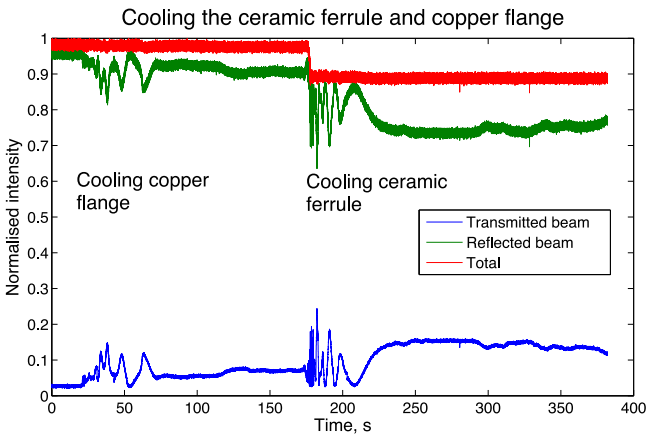

FIG. 6. Cooling of the copper feedthrough. Fluctuations of about 15% of the intensity of the transmitted component were observed but there was no overall drop in the intensity when the feedthrough was cooled.

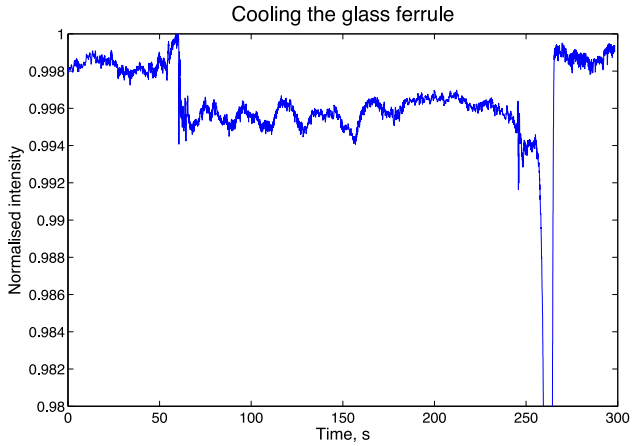

FIG. 7. Experimental results from testing the glass ferrule at liquid nitrogen temperatures. There is a small drop in the intensity of the transmitted component of 0.6%.

ferrule and the results are shown in Figure 7. Figure 7 shows a very small change in intensity of the transmitted beam, of approximately 0.6%, and a glass ferrule is now being used to terminate the fiber feed.

A low-stress hermetic feedthrough has also been developed which is based on the concept of Butterworth *et al.*[15] and uses vacuum grease to form the hermetic seal. By removing a few mm portion of the acrylate buffer layer from the fiber, an hermetic seal can be formed between the fiber and the steel tube, using Dow Corning© vacuum grease, as shown in Figure 8. This low-stress feedthrough has been hermetically tested at liquid nitrogen temperatures. This involved initially using attaching the flange to a vacuum vessel which was cooled by LN2 vapour, followed by immersion in LN2, while running a helium leak-detector. It has also been tested for stress at liquid nitrogen temperatures using the lab setup shown in Figure 3. Here, a stripped length of fiber is fed through the flange, and the output intensity in the desired polarisation is monitored while the flange is cooled by LN2 vapour followed by immersion in LN2. The resulting intensity is shown in Figure 9. The first cooling cycle produced a loss of intensity of 5%-7%, while subsequent cooling produced a loss of less than 2%.

The fiber termination and cryogenic feedthrough have been installed into the cryostat for the ISL experiment, which

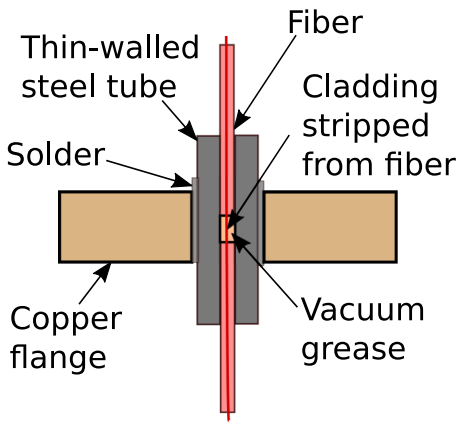

FIG. 8. Low-stress cryogenic feedthrough.

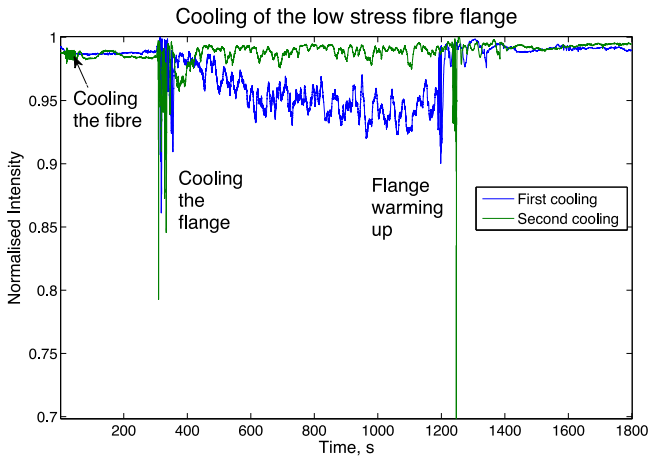

FIG. 9. Measured total intensity while cooling the low-stress cryogenic feedthrough. The first cooling exhibited a higher level of stress than subsequent coolings.

is cooled by immersion in LN2 and, subsequently, LHe in a 60 l Dewar. The flange is cooled over a period of minutes by conduction through the copper instrument housing (the bottom of which is first exposed to the liquid cryogen, while the flange is at the top of the housing). The termination of the fiber, inside the instrument housing, is cooled over a period of tens of minutes by a pressure of about 0.1 mbar (at room temperature) of helium exchange gas. The data shown are from a cooling cycle in which the inside of the experiment was only cooled as far as 8 K, but similar performance was observed at 4 K with a levitating float rather than a fixed mirror. The interferometer is a polarization-based interferometer whose input is a polarizing beamsplitter.[5] The angular motion detected by the interferometer is unaffected by variations of a few percent in intensity of input light, but the large changes in intensity observed initially with glued vacuum seals caused the interferometer to cease functioning reliably. The sensitivity required by the ISL experiment was achieved with the new fiber feed-through assembly at a temperature of 8 K, as shown in the noise spectrum in Figure 10. After the effects of variations in the input polarization have been sufficiently reduced, the noise at low frequency is dominated by 1/f noise in the readout electronics.

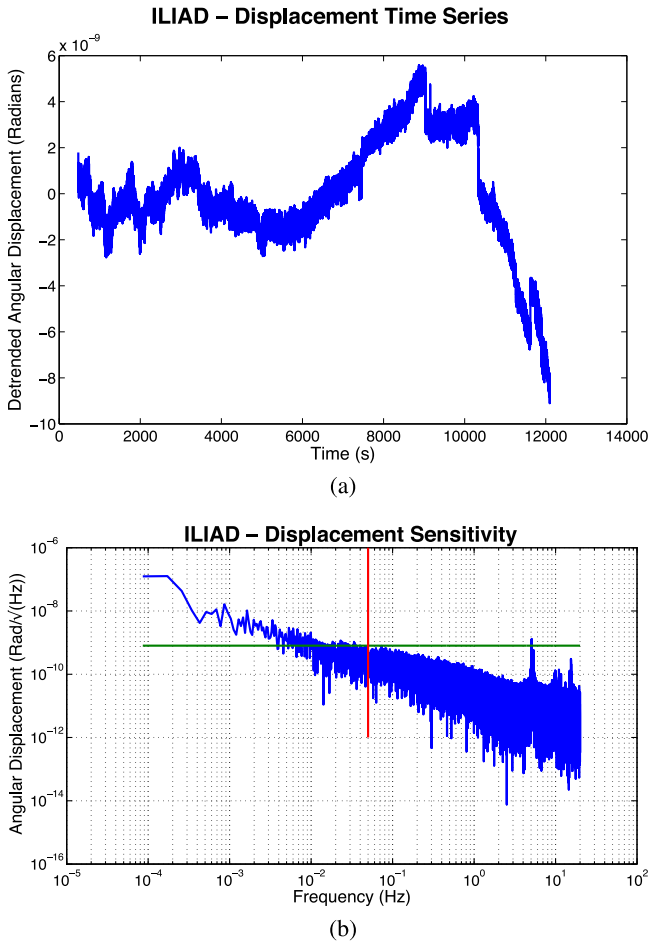

FIG. 10. (a) Time series during cryogenic operation of the homodyne polarization-based angular interferometer (ILIAD) at 8 K. (b) Sensitivity of the homodyne polarization-based interferometer (ILIAD) at 8 K. The cross shows the target sensitivity required for the ISL experiment.

V. CONCLUSION

Using a PM fiber, a homodyne interferometer can be operated in a vacuum at LHe temperature and sensitivities of 8×10^{-10} rad/$\sqrt{\text{Hz}}$ at a frequency of 0.2 Hz have been demonstrated. The observed TIBI can be modeled using a simple Jones matrix techniques and can be minimized by accurately aligning the input light with the fiber axis, reducing the stress in the feedthroughs and by replacing the ceramic ferrule which terminates the fiber with a glass ferrule.

This technology could easily be transferred to any weak-force cryogenic experiment in which small movements are to be measured, such as AFM measurements of surface structure and Casimir force measurements, and would allow capacitance measurements to be replaced by more accurate optical interferometric measurements.

Further work is underway to replace the cryogenic feedthrough with a more robust engineering solution in which the seal formed by vacuum grease is replaced by a seal in which the fiber is glued into a thick glass capillary tube, which is in turn glued into a thin-walled steel vacuum tube. By positioning the point at which the fiber is glued into the capillary sufficiently far from the metal components, it can be ensured that almost no stress is transferred to the fiber.

ACKNOWLEDGMENTS

We would like to thank the UK Science and Technology Facilities Council for their support for this project. We are also grateful to David Hoyland and John Bryant for their assistance in carrying out this work.

[1]E. Collett, *Polarized Light in Fiber Optics* (The PolaWave Group, 2003).
[2]E. C. Chalkley, S. M. Aston, C. J. Collins, M. J. Nelson, and C. C. Speake, in *Proceedings of the XLVI th Rencontres de Moriond and GPhyS Colloquium* (Gioi, 2011), p. 207.
[3]N. Arkani-Hamed, S. Dimopolous, and G. Dvali, "The hierarchy problem and new dimensions at a millimeter," Phys. Lett. B **429**, 263 (1998).
[4]G. H. Hammond, C. C. Speake, C. Trenkel, and A. P. Paton, "New constraints on short-range forces coupling mass to intrinsic spin," Phys. Rev. Lett. **98**, 081101 (2007).

[5]F. E. Pena-Arellano, H. Panjwani, L. Carbone, and C. C. Speake, "Interferometric measurement of angular motion," Rev. Sci. Instrum. **84**, 043101 (2013).
[6]R. H. Stolen, V. Ramaswamy, P. Kaiser, and W. Pleibel, "Linear polarization in birefringent single-mode fibers," Appl. Phys. Lett. **33**, 699 (1978).
[7]R. Paschotta, *Field Guide to Optical Fiber Technology* (Bellingham, Wash, 2010).
[8]G. P. Agrawal, *Nonlinear Fiber Optics* (Elsevier, 2006).
[9]J. Noda, K. Okamoto, and Y. Sasaki, "Polarization-maintaining fibers and their applications," J. Lightwave Technol. **4**, 1071 (1986).
[10]W. C. Young, *Roark's Formulas for Stress and Strain, Table 28*, 6th ed. (McGraw-Hill, New York, 1989).
[11]J. M. Senior, *Optical Fiber Communications* (Prentice-Hall International, 1985).
[12]F. Zhang and J. W. Y. Lit, "Temperature and strain sensitivity measurements of high-birefringent polarization-maintaining fibers," Appl. Opt. **32**(13), 2213 (1993).
[13]M. J. Marrone and M. A. Davis, "Low temperature behaviour of high-birefringence fiber," Electron. Lett. **21**, 16 (1985).
[14]D. Lee, P. R. Haynes, and D. J. Skeen, "Properties of optical fibres at cryogenic temperatures," MNRAS **326**, 774–780 (2001).
[15]J. S. Butterworth, C. R. Brome, P. R. Huffman, C. E. H. Mattoni, D. N. McKinsey, and J. M. Doyle, "A demountable cryogenic feedthrough for plastic optical fibers," Rev. Sci. Instrum. **69**, 3697 (1998).